Surface Plasmons

Lainey Ward
18365881
13/03/2021

Abstract

The phenomenon of surface plasmon resonance is demonstrated using the Kretschmann configuration with a thin silver film. The critical and plasmon resonance angles of a glass prism are determined with high accuracy for both red and blue light. The dielectric constant of the silver film is found to be $(-8.63 \pm 0.12) + i(0.33 \pm 0.00)$ and $(-3.84 \pm 0.01) + i(0.16 \pm 0.00)\ F/m$ for red and blue light, respectively. Using the dispersion relation, it is shown that the perpendicular propagation length is greater into the prism than into the metal. The phenomenon of Brewster's angle is also investigated for which the experimental findings align with the Fresnel equations.

1 Introduction

The Kretschmann configuration is used with a thin metal film to demonstrate the phenomenon of surface plasmon resonance (SPR).

A polarised electromagnetic (EM) wave strikes a dielectric-metal interface along which free electrons exist in a plasma state. At the interface, the EM wave excites surface plasmons (SPs) resulting in the production of a surface plasmon polariton (SPP) wave. The SPP partially reflects and refracts in both the dielectric and the metal. Within a few degrees of the critical angle (θ_c) of the dielectric, the intensity of reflected light obtains a minimum. This coincides with the maximum resonance of SPs.[1]

The incident angle at which SPR occurs (θ_r) depends on the wavelength and the polarisation of the incident light, as well as the metal thickness and type of media involved.

2 Theory

2.1 Electromagnetic Waves

An EM wave propagates through space via orthogonal oscillations of electric and magnetic fields. EM waves propagate at the speed of light (c) in a vacuum and at a reduced speed through other media. Upon striking a surface, an EM wave may be reflected, refracted, polarised or transmitted, all of which are pertinent to the Kretschmann configuration.

2.2 Polarisation

The polarisation of an EM wave refers to the orientation of its electric and magnetic fields. In linear polarisation, the electric and magnetic field vectors are confined to a single plane along the direction of propagation.

P- and S-polarised light refer to the confinement of the electric field vector to the plane parallel and perpendicular to the plane of incidence, respectively. P- and S-polarised EM waves are also commonly referred to as transverse-magnetic (TM) and transverse-electric (TE).[2]

2.3 Brewster's Angle

Brewster's angle (θ_B) is the angle of incidence at which the transmittance of polarised light through a transparent dielectric surface is maximised. At this angle, the reflection of the polarised light is also minimised. Therefore, at θ_B, unpolarised light becomes almost perfectly polarised.

θ_B is derived using Snell's law and expressed as follows:[2]

$$\theta_B = \tan^{-1}\left(\frac{n_2}{n_1}\right) \tag{1}$$

with n_2, the refractive index of medium 2, and n_1, the refractive index of medium 1.

The fraction that is reflected and transmitted can be determined by the Fresnel equations, and is a function of the incident angle (θ_{in}) and polarisation. The Fresnel, reflectance and transmittance equations are given in Section 6.1 and predict that approximately no P-polarised light is reflected at θ_B.[2]

2.4 Surface Plasmon Polaritons

Metals are good electric conductors and therefore have free electrons that do not remain permanently associated with their atoms. Such 'delocalised' electrons form a gas cloud known as the free electron gas density around the metal boundaries.

SPs are collective electron oscillations within the free electron gas density. When SPs couple with a photon or electron they become excited and produce an SPP. SPP refers to the entire excitation of the SP oscillations and the EM wave. They are always P-polarised longitudinal waves.[1]

In the case of photon excitation, an intermediate dielectric is placed between the air and metal to ensure SPR occurs. Such conditions are discussed in detail in Section 2.7.

2.5 Dielectric Function

The dielectric constant (ϵ) is the ratio of the electric permeability of a medium to that of free space. It is a function of state variables including frequency, temperature and pressure.

The dielectric constants for the metal ($j = 1$) and dielectric ($j = 2$) consist of a real and imaginary part where:

$$\epsilon_j = \epsilon_j' + i\epsilon_j'' \quad j = 1, 2 \tag{2}$$

However, for noble metals such as silver it is acceptable to assume that the imaginary parts of ϵ_2 are relatively small such that they may be neglected.[3]

The imaginary part of ϵ_1 can be expressed in terms of the refractive index of the metal (n_m) where:[4]

$$\epsilon_1'' = \sqrt{4\left(n_m^2 - \frac{\epsilon_1'}{2}\right)^2 - \epsilon_1'^2} \tag{3}$$

2.6 Wave Vector

The metal–dielectric interface can be considered in the $z = 0$ plane, parallel to the x-axis, with the metal at $z < 0$ and the dielectric at $z > 0$. From Maxwell's equations it can be shown that the SPP wave vector (k) has components along both the x- and z-planes.

In-Plane

The in-plane component of the wave vector (k_x) of an SPP is complex. k_x is also known as the dispersion relation and is given by:[1]

$$k_x = k_x' + ik_x'' \tag{4}$$

where :

$$k_x' = \left(\frac{\epsilon_1'\epsilon_2}{\epsilon_1' + \epsilon_2}\frac{w^2}{c^2}\right)^{\frac{1}{2}} \tag{5}$$

and:

$$k_x'' = \left(\frac{\epsilon_1'\epsilon_2}{\epsilon_1' + \epsilon_2}\right)^{\frac{1}{2}} \frac{\epsilon_1''\epsilon_2}{2\epsilon_1'(\epsilon_1' + \epsilon_2)}\frac{w}{c} \tag{6}$$

The real part of k_x determines the SPP wavelength and is determined from Eq. 5 as follows:[3]

$$\lambda_{spp} = \frac{2\pi}{k_x'} = \left(\frac{\epsilon_1' + \epsilon_2}{\epsilon_1'\epsilon_2}\right)\lambda \tag{7}$$

With λ, the wavelength of the incident EM wave in free space.

The imaginary part of k_x accounts for the damping of the SPP as it propagates along the interface. The propagation length is the distance for the electric field to decrease by a factor of 1/e and is equal to $1/(k_x'')$. This exponential damping is caused by ohmic losses of the SPP electrons and results in heating of the metal. The propagation length is approximately 30 μm for red light incident on a silver film (assuming the dielectric is air).[3]

Out-of-Plane

The out-of-plane component of the wave vector (k_z) is given perpendicularly into the metal:

$$k_{1,z} = \sqrt{\frac{\epsilon_1'^2}{\epsilon_1' + \epsilon_2}}\left(1 + i\frac{\epsilon_1''}{2\epsilon_1'}\right)\frac{w}{c} \tag{8}$$

and into the dielectric:

$$k_{2,z} = \sqrt{\frac{\epsilon_2^2}{\epsilon_1' + \epsilon_2}}\left(1 - i\frac{\epsilon_1''}{2(\epsilon_1' + \epsilon_2)}\right)\frac{w}{c} \tag{9}$$

The propagation length along the z-plane is $1/(k''_{j,z})$. Using the same parameters for silver as before, the propagation length into the metal and dielectric are 23 and 421 nm, respectively. Therefore the decay of the SPP into the dielectric is greater than into the metal.

2.7 Excitation Conditions

In order to excite SPPs, energy and momentum must be conserved. The conditions for successful SPP excitation are:

- The k_x values must be equal for the SPP and the incident EM wave. For a given frequency, the SPP k_x vector is always greater than that of an EM wave in free space. Due to this mismatch, an SPP cannot be directly excited by light propagating in free space. Therefore, excitation is only possible if the k_x of the incident light is increased from its free space value.[3] The most simple solution is the use of a dielectric with a refractive index greater than free space such as a prism.
- A non-zero real k_x is required. It is evident from Eq. 7 that this condition is only fulfilled if:[1]

$$\epsilon_1 \epsilon_2 < 0 \tag{10}$$

and:

$$\epsilon_1 + \epsilon_2 < 0 \tag{11}$$

These boundary conditions imply that one of the dielectric constants must be negative with an absolute value greater than the other. Therefore, the dielectric function must change sign across the boundary in order to produce an SPP.[3]

S-polarised EM waves have a k_x value of zero and therefore they do not attain these requirements.

2.8 Resonance

SPR refers to the maximum excitation of SPPs and occurs when the k_x components of the SPP and the incident EM wave are most equal. k_x of the incident light may be adjusted by changing the angle of incidence on the dielectric. The angle at which this occurs is the resonance angle (θ_r).[1]

SPR is represented by a minimum in the intensity of reflected light. This minimum occurs as most of the incident light energy has been converted into SPPs at the interface. It is also partially due to destructive interference between the SPPs and the internally reflected light.[3]

2.9 Historical Context

Recently, the study of the electromagnetic response of metals has developed into a research field of its own called 'plasmonics'.

During the early 20th century, Robert Woods noticed that unusual dark bands appeared in a diffracted spectrum of polarised light. However, he could not provide scientific reasoning for this phenomenon. In 1941, Ugo Fano concluded that these dark bands were associated with surface waves, now known as SPPs.

In 1952, Otto Hahn demonstrated the excitation of surface plasmons by means of attenuated total reflection. In the same year, Erich Kretschmann and Heinz Raethers supported these findings using a different configuration. This configuration is adopted in the experimental method in Section 3.1.

Simultaneously, David Pines and David Bohm suggested that energy losses in thin foils could be accounted for by the excitation of conducting electrons. Rufus Richie first coined the term 'surface plasmons' in 1957. He further developed the work of Pines and Bohm to include the interaction of the plasma oscillations with the surfaces of metal foils.[5]

Following this work, interest in plasmonics has increased considerably, in particular for thin films. Today SPPs are utilised to measure the binding of molecules such as proteins in real-time, as well in thin film solar cells as for improved energy-absorption.[6]

3 Methods

3.1 Experimental Configuration

The Kretschmann configuration is used in the experiment, as illustrated in Fig. 1. A monochromatic He-Ne laser is the EM source, a right-angled glass prism is the dielectric, and a thin silver film is the metal. P- and S-polarisation is achieved by rotating a linear polarising film 90 °.

The laser beam is perpendicularly incident on the linear polariser. The light then strikes the prism face at an angle (θ_{ext}) and then strikes the hypotenuse face at an angle (θ_{in}). Both angles are measured with respect to the normal of the hypotenuse face. As discussed, a portion of the light produces SPPs, a portion transmits across the metal, and a portion internally reflects within the prism and is incident upon a Light Dependent Resistor (LDR).

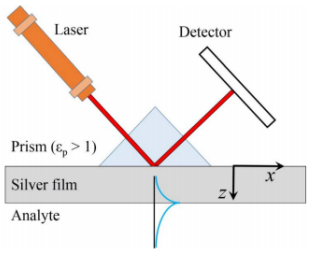

Fig. 1: Kretschmann configuration.

The LDR device operates on the principle of photoconductivity; its resistance is negatively proportional to both receiving light intensity and current. The LDR and a fixed resistor are set-up in a potential divider circuit. According to Ohm's law, an increase in the LDR resistance corresponds to an increase in the voltage drop across the LDR. Accordingly, the intensity on the LDR is proportional to its voltage (V_{ldr}). It follows that the voltage and intensity normalised (I_{ldr}/I_0) according to their maximum values are equal.

3.2 Voltage Acquisition

The LDR connects to a NI USB-6008 Data Acquisition (DAQ) device which is equipped with an Analog-to-Digital Converter (ADC). The voltage readings are obtained from the DAQ device and converted by the ADC using the attached Python code.

Within the code, the ADC channels are set to operate in differential mode. This offers a higher resolution and voltage range than single-ended mode.

3.3 Angle Acquisition

The prism itself sits on a rotating stage, encompassed by a larger rotating stage on which the LDR sits. Both stages are controlled by stepper motors which in turn are controlled by Python code. The stepper motors rotate through a fixed angle when a DC voltage is applied to its terminal.

To ensure that the LDR aligns with the reflected light, the larger stage is calibrated to rotate at some multiple of the radial frequency of the smaller stage. Both stages are rotated counterclockwise in the direction of increasing θ_{ext}.

The θ_{ext} is related to θ_{int} using the following equation:

$$\theta_{int} = sin^{-1}\left(\frac{sin(\theta_{ext} - A)}{n_p}\right) + A \qquad (12)$$

with A, the acute internal angle of the prism (45 °), and n_p, the refractive index of the prism.

The angle and voltage acquisition Python codes are combined within a function to ensure a voltage reading and the corresponding angle are obtained for every rotation of the stepper motors.

3.4 Experimental Method

The experiment is undertaken in 3 stages using red, blue, P- and S-polarised light.

Firstly, the maximum intensity of the lasers is obtained to enable the normalisation of intensity throughout the analysis. The laser is placed at an incident angle to the detector, with all other elements of the experimental set-up removed. An incident angle (θ_{in}) of 180 ° corresponds to the laser beam perpendicularly incident on the detector. V_{ldr} values are obtained over a range of θ_{in} for both red and blue light.

Secondly, V_{ldr} values are obtained over a range of θ_{ext} for P-polarised red and blue light using the experimental configuration described in Section 3.1.

Finally, V_{ldr} values are obtained over a range of θ_{in} for both P- and S-polarised red light incident on a flat glass.

3.5 Theoretical Values

The wavelengths of the red and blue laser are taken to be 632.8 and 442.0 nm, respectively.

The type of glass of the prism is unknown. However, BK4 glass is popular in laboratory-grade lenses and prisms. Assuming the prism is composed of Schott N-BK7 glass, n_p is approximately 1.515 for the red laser and 1.526 for the blue laser. Similarly, n_m is 0.0056 and 0.0400.

The dielectric constant of such a prism is $-(18.281 + i0.481)$ and $-(6.613 + i0.0206)$ F/m for the red and blue lasers, respectively.

4 Results & Analysis

Raw data and the propagation of uncertainty can be found within the attached Python document.

4.1 Red Laser: Calibration

V_{ldr} and θ_{in} values are obtained for the P-polarised red He-Ne laser directly incident on the LDR. For each θ_{in}, V_{ldr} is taken as the mean of 100 samples and the uncertainty is the standard deviation of these samples.

V_{ldr} is plotted against θ_{in} in Fig. 2. Using an Orthogonal Distance Regression (ODR) model, the data is fit to a quadratic function with estimated parameters:

$$y \approx (-0.04 \pm 0.01)x^2 + (15.67 \pm 2.03)x - (1403.74 \pm 183.31) \quad (13)$$

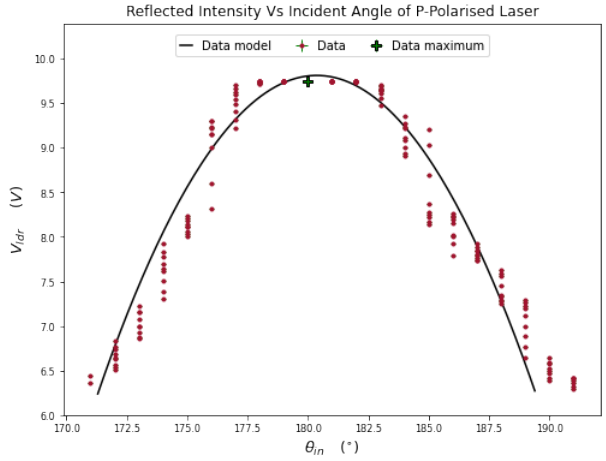

Fig. 2: Voltage plotted against the incident angle of a red P-polarised laser on an LDR.

The data model has an adequate coefficient of determination ($R^2 = .812$), implying that it predicts 85.2 % of the variance in V_{ldr}.

The maximum of Fig. 2 occurs at $(\theta_{in}, V_{ldr}) = (180.3 \pm 0.1\ °,\ 9.75 \pm 0.00\ V)$. In theory, the maximum occurs at 180°. Therefore, the experimental maximum has a low percent error of 0.14 %, indicating a high degree of accuracy.

4.2 Blue Laser: Calibration

Section 4.1 is repeated for the blue He-Ne laser.

V_{ldr} is plotted against θ_{in} in Fig. 3 and the data is fit to a quadratic function with estimated parameters:

$$y = -(0.04 \pm 0.00)x^2 + (15.03 \pm 0.26)x - (1343.97 \pm 23.66)$$

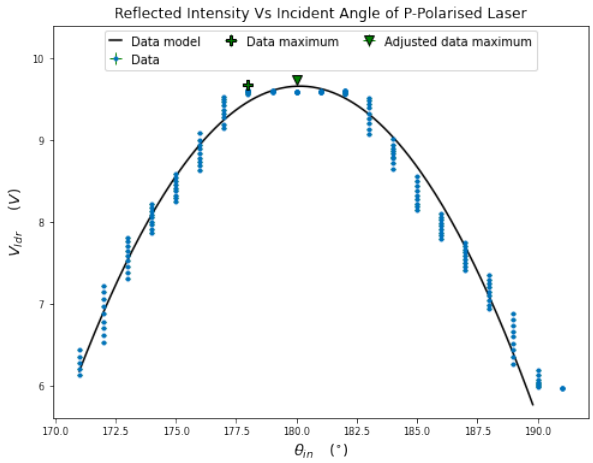

Fig. 3: Voltage plotted against the incident angle of a blue P-polarised laser on an LDR.

The data model has a high coefficient of determination ($R^2 = .933$), implying that it predicts 93.3 % of the variance in V_{ldr}.

The maximum of Fig. 3 occurs at $(\theta_{in}, V_{ldr}) = (178.0 \pm 0.1\ °,\ 9.61 \pm 0.00\ V)$. However, the data concaves towards the centre of the plot, likely due to oversaturation of the LDR. To recify this error, the maximum data point is horizontally readjusted to occur at $\theta_{in} = (180 \pm 0.10)\ °$ and vertically readjusted by 0.6 V to align closer with that predicted by both the data model and the maximum in Fig. 2. The final maximum occurs at $V_{ldr} = (9.67 \pm 0.00)\ V$, slightly lower than that in Fig. 2.

4.3 Red Laser: Kretschmann

LDR voltage and θ_{ext} values are obtained from the DAQ device for the P-polarised red He-Ne laser using the Kretschmann configuration. Once again, for each θ_{ext}, V_{ldr} is taken as the mean of 100 samples and the uncertainty is the standard deviation of these samples. 5 data sets are taken, across which the mean voltage and uncertainty are determined.

V_{ldr} is normalised (I_{ldr}/I_0) according to the maximum V_{ldr} from Section 4.1. The θ_{ext} values are converted to θ_{int} using Eq. 12.

I_{ldr}/I_0 is plotted against θ_{int} in Fig. 4 and fitted with a univariate spline. The plot depicts a discontinuity along the leftmost side followed by a sharp minimum.

θ_c coincides with the plot maximum and occurs at $(\theta_{in}, V_{ldr}) = (41.82 \pm 0.03\ °,\ 0.99 \pm 0.00\ V)$. Using Eq. 22, the theoretical θ_c is determined to be 41.27 °.

The experimental θ_c has a low percent error of 1.3 %.

Substituting the experimental θ_c value into Eq. 22 returns a value for the prism refractive index of (1.50 ± 0.00). This has a very low percent error of -0.01 % with respect to that of BK7 crown glass with incident wavelength of 632.8 nm. However, it should be noted that the conversion of θ_{ext} into θ_{int} requires substitution of the theoretical refractive index. Therefore, the extent to which this increases the accuracy of θ_c requires further analysis.

θ_r coincides with the plot minimum and occurs at $(\theta_{in}, V_{ldr}) = (44.54 \pm 0.07\ °, 0.91 \pm 0.00\ V)$.

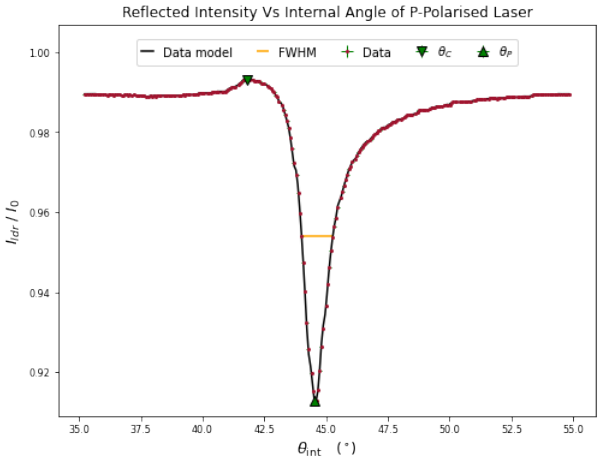

Fig. 4: Normalised reflected intensity plotted against the internal angle of a red P-polarised laser in a prism.

By rearranging Eq. 3, 5 and 6, the experimental ϵ_1 for an incident red laser is found to be $(-8.63 \pm 0.12) + i(0.33 \pm 0.00)\ F/m$. It should be noted that ϵ_1'' is calculated by substituting the theoretical value of n_m into Eq. 3, as its experimental value is undetermined. The real and imaginary parts of ϵ_2 have high percent errors of -52.8 % and -31.3 %, respectively.

Using Eq. 7, the theoretical and experimental λ_{spp} are determined to be 615.2 and $(595.0 \pm 6.5)\ nm$, respectively. The experimental value has a low percent error of -3.29 %. This high accuracy is surprising given the low accuracy of ϵ_1' and that it is the only experimental variable within Eq. 7.

Using Eq. 5, 8 and 9, the experimental propagation lengths parallel to the interface and perpendicular to the interface towards the dielectric and metal are calculated to be 37.8, 1.68 and 12.9 μm, respectively. For simplicity, the dielectric is taken as air ($\epsilon_2 = 1.005$). As discussed in Section 2.6, the propagation into the metal is much shorter than into the dielectric.

4.4 Blue Laser: Kretschmann

Section 4.3 is repeated for the blue He-Ne laser. The method of calculation of all values remains the same. However, V_{ldr} is normalised using the maximum V_{ldr} value in Section 2.2.

I_{ldr}/I_0 is plotted against θ_{int} in Fig. 5. It is immediately apparent that the plot is more exaggerated and horizontally broadened that in Fig. 4. The full width at half maximum is a factor of 8.51 greater for the blue laser.

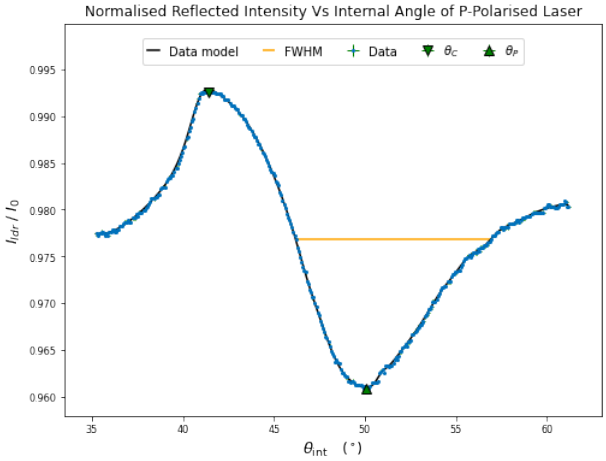

Fig. 5: Normalised reflected intensity plotted against the internal angle of a blue P-polarised laser in a prism.

The theoretical θ_c is determined to be 41.27 °. θ_c occurs at $(\theta_{in}, V_{ldr}) = (41.40 \pm 0.01\ °, 0.99 \pm 0.00\ V)$ in Fig. 5, with a low percent error of 0.3 %.

Substituting this value into Eq. 22 returns a value for the prism refractive index of (1.50 ± 0.00), similar to that for the red laser. This has a percent error of ≈ 0.0 % with respect to that of BK7 crown glass with incident wavelength of 442.0 nm.

θ_r occurs at $(\theta_{in}, V_{ldr}) = (50.09 \pm 0.04\ °, 0.96 \pm 0.00\ V)$. The experimental ϵ_1 for an incident blue laser is found to be $(-3.84 \pm 0.01) + i(0.16 \pm 0.00)\ F/m$. The real and imaginary parts of ϵ_1 have comparable percent errors to the red laser with -42.0 % and -23.8 %, respectively.

The theoretical and experimental λ_{spp} are determined to be 407.2 and $(380.0 \pm 0.9)\ nm$, respectively, with a percent error of -6.7 %. This high accuracy is surprising given the low accuracy of ϵ_1' and that it is the only experimental variable within Eq. 7.

Finally, the experimental propagation lengths

parallel to the interface and perpendicular to the interface towards the dielectric and metal are calculated to be 8.4, 1.5 and 4.3 μm, respectively. Once again, the propagation into the metal is much shorter than into the dielectric.

4.5 Comparison: Kretschmann

θ_c is plotted against θ_r in Fig. 6. Using an ODR, the two points are fit to a linear function with estimated parameters:

$$y = -(20.2 \pm 0.0)x + (887.4 \pm 0.0) \tag{14}$$

Ideally, the experiment should be repeated for more laser wavelengths, in order to determine the significance of the relationship between λ, θ_r, and θ_c.

From the plot it can be inferred that there is a negative correlation between θ_r and θ_c, and a positive correlation between θ_c and λ. The latter aligns with Eq. 23.

Furthermore, θ_c should be a factor of $632.8/442 \approx 1.43$ greater for red light than blue. The experimental factor is found to be 1.01, corresponding to a percent error of -29.4 %.

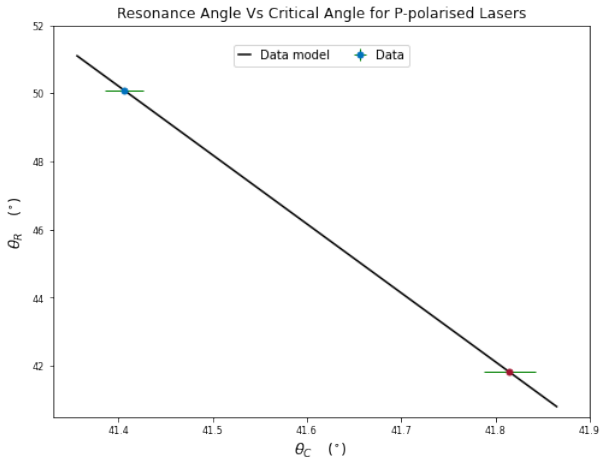

Fig. 6: SP resonance angle plotted against prism critical angle of the red and blue P-polarised lasers.

In Section 4.3 and 4.3 is is found that the real part of ϵ_2 is smaller for the red laser than the blue. It can be concluded that ϵ_2 is negatively proportional to λ for a given metal thickness.

Similarly, the propagation lengths parallel and perpendicular to the metal-dielectric interface are greater for the red laser than the blue and so the propagation lengths are proportional to λ.

It is also notable that the experimental values for ϵ_2 and n_p are all less than their (assumed) true values.

4.6 P-Polarised

V_{ldr} and θ_{in} values are obtained for the P-polarised red He-Ne laser incident on a flat glass. For each θ_{in}, V_{ldr} is taken as the mean of 100 samples and the uncertainty is the standard deviation of these samples.

I_{ldr}/I_0 is plotted against θ_{in} in Fig. 7 and the data is fit to a univariate spline. The minimum in the plot coincides with θ_B and occurs at $(57.2 \pm 0.1\ °, 0.23 \pm 0.00)\ V$. θ_B has a low percent error of 1.1 %, relative to the theoretical value of 56.6 °. It is assumed the flat glass has the same refractive index as the prism.

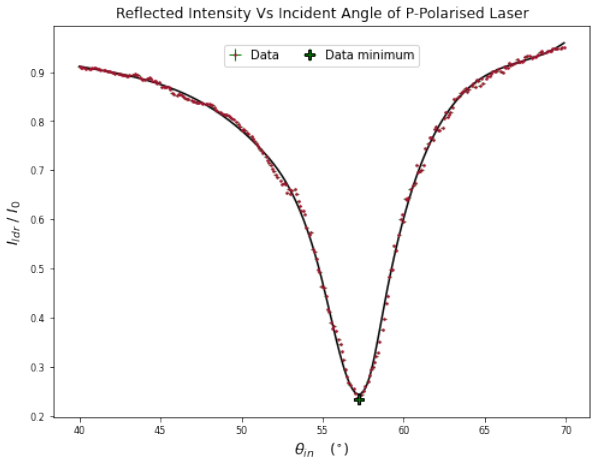

Fig. 7: Normalised reflected intensity plotted against the incident angle of a red P-polarised laser on a flat glass

Fig. 7 confirms that the reflected intensity reduces significantly at θ_B, implying that the majority of the incident light is transmitted within the flat glass.

This is further confirmed by the experimental values returned by Eq. 16 - 21, according to which the percentage of reflected and transmitted P-polarised light is 0.01 % and 99.99 % at θ_B. I_{ldr}/I_0 does not reduce to exactly zero in Fig. 7 due to ambient light incident on the LDR. The experiment should be conducted in total darkness to minimise this offset.

4.7 S-Polarised

Section 4.6 is repeated for red S-polarised light. I_{ldr}/I_0 is plotted against θ_{in} in Fig. 8.

In contrast to Fig. 7, no distinct minimum features in the plot. Instead, there is a significant positive

linear correlation ($r = .989,\ p < .001$) between I_{ldr}/I_0 and θ_{in}.

The data is fit to a linear ODR model with estimated parameters:

$$y = -(20.2 \pm 0.0)x + (887.4p) \tag{15}$$

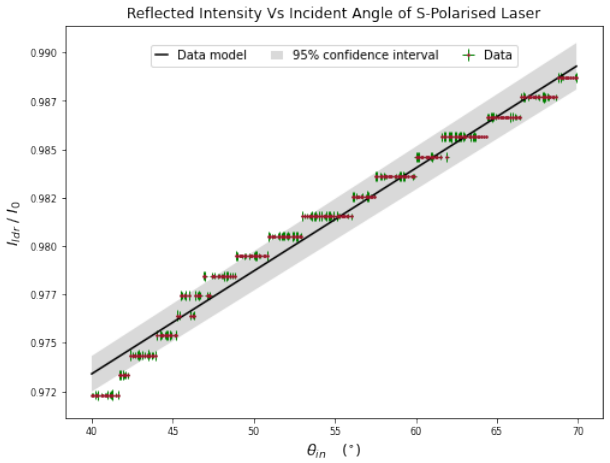

Fig. 8: Normalised reflected intensity plotted against the incident angle of a red S-polarised laser on a flat glass.

Once again, using the experimental values for θ_B and n_p and the Fresnel equations, the percentage of reflected and transmitted S-polarised light is 15.4 % and 84.6 %.

4.8 Further Investigation

There are many other characteristics of SPPs that warrant further analysis. Many of these investigations are easily realizable within the Kretschmann configuration.

For example:

- A well-worn prism could be used to investigate the effects of surface imperfections on the production of SPPs.
- Silver films of varying thickness could be used to investigate the relationship between thickness and the production of SPPs.
- I_{ldr}/I_0 could be plotted against θ_{in} for varying degrees of polarisation using a circular polariser. It is expected that the produced curves would be an intermediate of Fig. 7 and Fig. 8.
- It could be demonstrated that SPPs cannot be produced directly on a metal surface. Alternatively, a dielectric that does not have a negative dielectric constant could be used to demonstrate that the dielectric function must change sign across the interface.

5 Conclusion

The phenomenon of surface plasmon resonance is demonstrated and examined using the Kretschmann configuration with a thin silver film.

The critical and plasmon resonance angles of a glass prism are found to be $(41.8 \pm 0.0\ °,\ 44.5 \pm 0.0\ °)$ and $(41.4 \pm 0.0\ °,\ 50.1 \pm 0.0\ °)$ for red and blue light, respectively. The experimental critical angles both have percent errors < 1.3 % relative to their theoretical values.

A negative linear relationship of unknown significance is determined between critical and resonance angle, and a positive relationship between critical angle and incident wavelength.

The dielectric constant for the silver film is determined to be $(-8.63 \pm 0.12) + i(0.33 \pm 0.00)$ and $(-3.84 \pm 0.01) + i(0.16 \pm 0.00)\ F/m$ for red and blue light, respectively. Their corresponding propagation lengths are determined to lie within the range $(1.5, 37.8)\ \mu m$. It is also shown that the perpendicular propagation length is greater into the prism than into the metal.

The phenomenon of Brewster's angle is also investigated using a flat glass. It is shown that the majority of incident light is transmitted at an incident angle equal to Brewster's angle. A significant linear relationship is found between the intensity of reflected light and the incident angle. These experimental findings align with that predicted by the Fresnel equations.

Overall, plamonics is a complex field of study that lends itself to extensive experimental analysis, even within a simple Kretschmann configuration.

References

[1] J. Sambles, *Optical Excitation of Surface Plasmons: An Introduction*, vol. 32, pp. 2–9. Taylor and Francis Ltd, 1991.

[2] E. Hecht, *Diffraction*, ch. 4,8, pp. 124–130, 133, 338. Pearson, 5^{th} ed., 2017.

[3] *Surface Plasmons*, ch. 12, pp. 414–418. Swiss Federal Institute of Technology Zurich, 2017.

[4] *Plasmonics*, ch. 17, p. 209. Humboldt University of Berlin, 2017.

[5] *Brief History of the Technique*. Horiba.

[6] W. Wei, *Large Absorption Enhancement in Ultrathin Solar Cells Patterned by Metallic Nanocavity Arrays*. Scientific Reports, 2016.

6 Appendix

6.1 Fresnel Equations

The Fresnel equations for the reflection (r_s) and transmission (t_s) of S-polarised light and the reflection (r_p) and transmission (t_p) of P-polarised light are as follows:[2]

$$r_s = \frac{n_1 \cos\theta_i - n_2 \cos\theta_t}{n_1 \cos\theta_i + n_2 \cos\theta_t} \tag{16}$$

$$t_s = \frac{2n_1 \cos\theta_i}{n_1 \cos\theta_i + n_2 \cos\theta_t} \tag{17}$$

$$r_p = \frac{n_2 \cos\theta_i - n_1 \cos\theta_t}{n_2 \cos\theta_i + n_1 \cos\theta_t} \tag{18}$$

$$t_s = \frac{2n_1 \cos\theta_i}{n_2 \cos\theta_i + n_1 \cos\theta_t} \tag{19}$$

The reflectance (R) is the ratio of the reflected to incident EM power and can be determined for S- and P-polarised components separately:

$$R_{s,p} = |r_{s,p}|^2 \tag{20}$$

Similarly, the transmittance (T) is:

$$T_{s,p} = 1 - R_{s,p}^2 \tag{21}$$

6.2 Critical Angle

The critical angle is defined as:[2]

$$\theta_c = \sin^{-1}\left(\frac{n_2}{n_1}\right) \tag{22}$$

Using the relation $n_1\lambda_1 = n_2\lambda_2$ and substituting into Eq. 22 gives:

$$\theta_c = \sin^{-1}\left(\frac{\lambda_1}{\lambda_2}\right) \tag{23}$$

where $\lambda_2 < \lambda_1$.